RESEARCH ARTICLE

Applied Polymer WILEY

Effect on thermal, mechanical, and biodegradable properties of plasma-treated fish scale powder/linear low-density polyethylene polymer composite films

Matthew Bonzu Ackah | Radhika Panickar | Vijaya K. Rangari 🗅

Department of Materials Science Engineering, Tuskegee University, Tuskegee, Alabama, USA

Correspondence

Vijaya K. Rangari, Department of Materials Science Engineering, Tuskegee University, Tuskegee, AL 36088, USA. Email: vrangari@tuskegee.edu

Funding information

Alabama EPSCoR, Grant/Award Number: 1655280; NSF-CREST, Grant/Award Number: 1735971; MRI, Grant/Award

Number: 2117242

Abstract

In the present work, we report the effect of low-temperature plasma treatment on thermal, mechanical, and biodegradable properties of polymer composite blown films prepared from carp fish scale powder (CFSP) and linear low-density polyethylene (LLDPE). The CFSP was melt compounded with LLDPE using a filament extruder to prepare 1, 2, and 3 wt.% of CFSP in LLDPE polymer composite filaments. These filaments were further pelletized and extruded into blown films. The blown films extruded with 1, 2, and 3 wt.% of CFSP in LLDPE were tested for thermal and mechanical properties. It was observed that the tensile strength decreased with the increased loading content of CFSP, and 1% CFSP/LLDPE exhibited the highest tensile strength. To study the effect of low-temperature plasma treatment, 1% CFSP/LLDP polymer composite with high tensile strength was plasma treated with O₂ and SF₆ gas before blow film extrusion. The 1% CFSP/LLDPE/SF₆-extruded blown films showed increased thermal decomposition, crystallinity, tensile strength, and modulus. This may be due to the effect of crosslinking by the plasma treatment. The maximum thermal decomposition rate, crystallinity %, tensile strength, and modulus obtained for 1% CFSP/ LLDPE/SF₆ film were 500.02°C, 35.79, 6.32 MPa, and 0.023 GPa, respectively. Furthermore, the biodegradability study on CFSP/LLDPE films buried in natural soil for 90 days was analyzed using x-ray fluorescence. The study showed an increase in phosphorus and calcium mass percent in the soil. This is due to the decomposition of the hydroxyapatite present in the CFSP/LLDPE biocomposite.

KEYWORDS

biodegradable, Fishscale powder, mechanical properties, thermogravimetric analysis (TGA), thermoplastics

1 | INTRODUCTION

Fish scales are one of animal-based bio fillers, which are usually generated by fish processing industries. Fish industries create a lot of fish waste during processing, with about 75 million tons of fish waste generated annually.¹ Disposing of fish waste commonly involves

dumping it in seas or landfills or incineration in the open air. The accumulation of fish waste gives off offensive odors and germinates bacterium, which can cause severe environmental and health issues.² Effectively utilizing fish waste will not only reduce the negative impact it has on the environment but also add commercial value. The main composition of the fish scale is the organic

component, encompassing collagen, fat, vitamins, and so forth, and the inorganic components consist of hydroxyapatite (HA) and other trace elements like calcium, zinc, and iron. HA, with a chemical composition of $(Ca_{10}(PO_4)_6(OH)_2)$, is embedded in the organic matrix of collagen in fish scales and is a promising reinforcing material for polymers due to its high stiffness and strength.

Fish scales' low cost, abundance, and availability have increased interest in utilizing fish scale powder (FSP) as a bio filler. FSP can be incorporated into polymer matrices to create biocomposites with improved properties.⁵ Incorporating FSP into polymer matrices to create biocomposites has potential applications in various industries such as packaging, construction, and biomedical engineering.⁶ Biocomposites from FSP can be biodegradable, mitigating negative environmental impact. To investigate the effect of FSP as bio filler in an epoxy matrix composite, Babu et al⁸ fabricated the composites using the hand lay-up method. They evaluated mechanical properties such as tensile, flexural, and impact strength and attained maximum tensile strength at a 30% volume fraction of fish scales and reported that further addition of fish scale filler resulted in reduced mechanical properties. The hardness of the composites, flexural strength, and density increased with increasing loading content of the catla fish scale. HA, a calcium phosphate mineral embedded in fish scale's collagen matrix provides hardness to the scales. Wang et al. 9 synthesized a HA/polyethylene composite and concluded that the composites had sufficient mechanical strength to find utility in bone regeneration. Majhooll et al. 10 studied adding fish scales HA powder to epoxy resin to create a composite and reported that 10 wt.% filler content had the highest flexural strength.

Plasma treatment serves to modify the surface of materials to achieve effective surface modification techniques to alter the surface properties of various materials without damaging the bulk material. It involves subjecting the material to a low-temperature plasma source to modify its surface at a temperature below the melting point. 11 Plasma treatment can properly introduce functional groups, graft polymerization, and enhance the crosslink formation of polymeric materials. 12 The functional groups introduced to the surfaces of materials by plasma treatment can activate the material's surface. Choi et al. 13 used oxygen plasma treatment to reveal reactive groups on a material surface for additional grafting of bioactive moieties. The oxygen plasma species generated on polyurethane films were subsequently employed for acrylic grafting. Similarly, Lee et al. 14 and Sartori et al.¹⁵ used plasma treatment to introduce carboxylic and COOH functional groups to the surface of polymeric and poly(ester urethane) films.

Many research works have been conducted and reported on biocomposites using FSP as a bio filler, however, no research work has been reported on the influence of plasma treatment on the properties of FSP-based biocomposites. The present work focuses on the preparation of different wt.% of (1,2, 3 wt.%) carp fish scale powder (CFSP) in linear low-density polyethylene (LLDPE) biocomposite using filament and blown film extrusion techniques. The optimized wt.% of CFSP/LLDPE biocomposite with improved thermal and mechanical properties was further subjected to lowtemperature plasma treatment with O2 and SF6 gases. The manuscript discusses the effect of plasma treatment on the mechanical, thermal, and biodegradable properties of CFSP/ LLDPE biocomposite films. It was understood that the effect of plasma in the biocomposite significantly improved the thermal, mechanical, and biodegradable properties of the CFSP/LLDPE biocomposite films.

2 | MATERIALS AND METHODS

2.1 | Materials

The materials used in this study, CFS were purchased from Nizona Inc., Mumbai, India. The fish scales were washed with distilled water and dried at in the oven. LLDPE, a product of ExxonMobil, was supplied by Premier Polymers LLC, Texas, USA. The density of the polymer resin was 0.917 g/cm³, and the melt flow was 2.0 g/10 min.

2.2 | Experimental

2.2.1 | FSP preparation

The CFS were crushed into powder using a cryo-milling machine (SpexSamplePrep, Freezer/Mill). The cryo-milling machine utilized liquid nitrogen, which froze and embrittled the fish scale, making it easier to grind into fine powder. The fish scales were precooled for 20 min and had a run time of 15 min for five cycles with a cooling time of 5 min. The total time taken was 2 h.

2.2.2 | Preparation of CFSP/LLDPE biocomposite filaments

The LLDPE and the CFSP were dry mixed in a plastic bag. Polyethylene glycol was utilized as a plasticizer and mixing agent. The selection of the dry mixing method aimed to save time and avoid using toxic reagents during biocomposite preparation. Three different compositions (1, 2, and 3 wt.%) of the CFSP in LLDPE were prepared.

A lower concentration of the CFSP was used because the higher concentration increased the viscosity of the LLDPE/CFSP during the extrusion process, making it difficult to extrude the film. Filabot ex2 filament extruder of dimensions 46 cm \times 18 cm \times 24 cm was used to filament extrude the dry mixed CFSP and LLDPE mixture. The extrusion of the CFSP/LLDPE biocomposite filaments was carried out at a temperature of 160° C, through a standard nozzle size of 1.75 mm. The extruded filament was pelletized and extruded again for the second time to ensure uniform dispersion of the blend.

2.2.3 | Plasma treatment of filament polymer biocomposite

The extruded filaments were chopped into pellet form and low-temperature plasma treated using custom-designed rotating drum PLASMA ETCH (Progress Through Innovation, Carson City, NV, USA), a machine with 150 Hz radio frequency-generated power. The optimized concentration of 1% CFSP/LLDP biocomposite that exhibited high mechanical strength was further exposed to low-temperature plasma treatments for 10 min in the presence of $\rm O_2$ and $\rm SF_6$ separately at 30 and 5 sccm, respectively.

2.2.4 | Preparation of CFSP/LLDPE biocomposite blown films

The pellets of polymer biocomposite were fabricated into blown films using an ultra-film micro-blowing line machine (LabTech) shown in Figure 1a. The extruder has a conical screw with a diameter of 18 mm at the feed and 8 mm at the end with a screw L/D ratio of 30. The pellets of different wt. % of CFSP in LLDPE were fed into the hopper, where the screw rotates and forces the material to flow through a die that makes a hollow blown film. The outside of the tube is an external air ring that cools the film down, and inside the tube is an air valve that introduces air into the bubble and helps control the diameter of the bubble while blowing the film. The bubble goes up through the guide rails and to the nip rolls, which ensures that a thin film is formed. The thin films go through a series of idle rollers before they are collected on the winding rollers to ensure continuous operation. The material was run at a screw and die temperature of 170°C. The screw speed was 65 rpm, and the external ring, which helps with the cooling of the film, was at 1300 rpm. The nip roll speed was set at

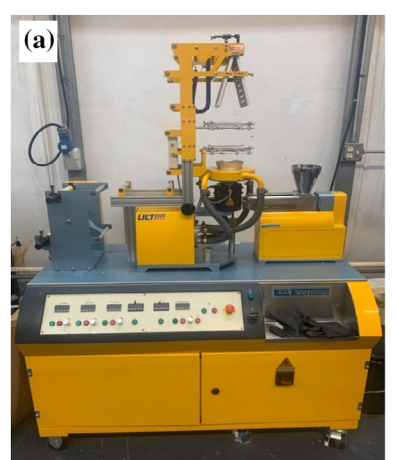




FIGURE 1 (a) Blow film machine used for biocomposite film extrusion and (b) 1 wt.% carp fish scale powder/SF₆ blown film prepared. [Color figure can be viewed at wileyonlinelibrary.com]

15.24 cm/min. The fabricated films had an average thickness of 0.18 mm, shown in Figure 1b. The sample names and weight percentages of the CFSP and LLDPE are given in Table 1.

2.2.5 | Biodegradability test

A natural soil burial test was used to examine the biodegradability of the biocomposite films. 1% CFSP/LLDPE, 1% CFSP/LLDPE/ O_2 , and 1% CFSP/LLDPE/ SF_6 films were buried in a soil.

The samples were replicated three times. A total of 9 pots with soil were set up as shown in Figure 2 and the pots were watered regularly to keep moisture. The samples were buried for 90 days before being them out for further x-ray fluorescence (XRF) analysis. Figure 2b shows the 1% CFSP/LLDPE/SF₆ films collected after 90 days of soil burial test for XRF analysis.

2.3 | Characterization

2.3.1 | Scanning electron microscopy

The morphology of the synthesized CFSP and the fractured surface of the LLDPE/CFSP biocomposite films after tensile strength were analyzed using JEOL JSM-7200F field emission scanning electron microscope (FESEM, JEOL USA, Peabody, MA). The samples were sputter coated with gold/palladium (Au/Pd) under Argon atmosphere for 5 min at 10 mA using a Hummer sputter coater before SEM analysis.

TABLE 1 Sample prepared for the present study.

			Plasma treatment with O ₂		Plasma treatment with SF ₆	
Sample	LLDPE (wt.%)	CFSP (wt.%)	Time (min)	Flow rate (sccm)	Time (min)	Flow rate (sccm)
Neat LLDPE	100	0	-		-	
1% CFSP	99	1	-		-	
2% CFSP	98	2	-		-	
3% CFSP	97	3	-		-	
1% CFSP/O ₂	99	1	10	30	10	5
1% CFSP/SF ₆	99	1	10	30	10	5

Abbreviations: CFSP, carp fish scale powder; LLDPE, linear low-density polyethylene.





FIGURE 2 (a) Image of the pots with the samples buried for biodegradability test and (b) 1% CFSP/LLDPE/SF₆ after burial test. CFSP, carp fish scale powder; LLDPE, linear low-density polyethylene. [Color figure can be viewed at wileyonlinelibrary.com]

2.3.2 | High-resolution transmission electron microscopy

Transmission electron microscopy (TEM) analysis was performed on the synthesized CFSP using the JOEL JSM-7200F FESEM transmission electron machine (FESEM, JEOL USA, Peabody, MA). The samples, prepared by dispersing the particles in ethanol, were placed on a copper grid and analyzed under the TEM.

2.3.3 | Fourier transform infrared spectroscopy

Fourier transform infrared (FTIR) spectrometer (IRTracer-100) with high resolution at 0.25 cm⁻¹ and high-speed scanning capable of 20 spectra/s was used to identify the compounds and functional groups in the

synthesized CFSP and fabricated LLDPE/CFSP biocomposite films.

2.3.4 | X-ray diffraction

The CFSP was analyzed using x-ray diffraction (XRD) studies using a Rigaku Smartlab x-ray diffractometer equipped with monochromatic radiation. The XRD was performed at a scan rate of 1° /min.

2.3.5 | Thermogravimetric analysis

Thermogravimetric analysis (TGA) was performed on the synthesized CFSP and LLDPE/CFSP biocomposite films using a TA Q500 thermogravimetric analyzer. The decomposition temperatures, weight change, and the

residue left were evaluated. The sample was placed on a platinum pan and heated at 10°C/min from 30 to 800°C under a nitrogen atmosphere.

2.3.6 | Differential scanning calorimetry

Thermal analysis of the LLDPE/CFSP biocomposite films was performed using differential scanning calorimetry (DSC) TA-Q series 2000 under a nitrogen atmosphere at a 10°C/min heating rate. The samples were heated from 30 to 300°C followed by cooling to 30°C.

2.3.7 | Tensile test

The uniaxial tensile tests were performed to analyze the mechanical properties of fabricated LLDPE/CFSP biocomposite films using a Zwick/Roell Z2.5 universal mechanical testing machine. A load cell of 2.5 kN was used, and the test was run at a crosshead speed of 50 mm/min with a preload of 0.1 MPa. The Zwick/Roell software associated with the machine calculated and provided results for Young's modulus, elongation at break, tensile strength, and force at break.

2.3.8 | Biodegradability test

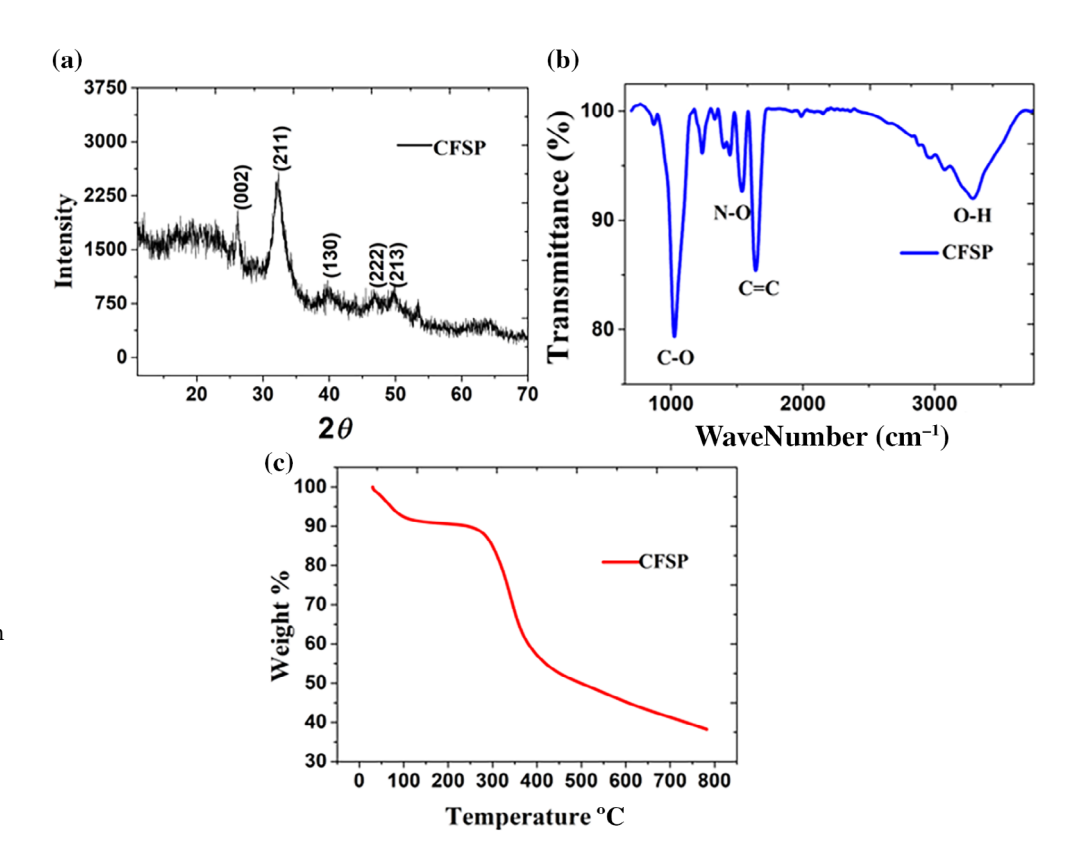
Rigaku NEX QC+ QUANTEZ advanced XRF with a 50 kV x-ray tube for elemental coverage was used to analyze the changes in the chemical composition of the soil before and after the natural soil burial test.

3 | RESULTS AND DISCUSSIONS

3.1 | Characterization of CFSP

The composition of the CFSP was analyzed using XRD, and Figure 3a shows the XRD pattern of CFSP exhibiting diffracted peaks at 2θ values of 24° and 32° corresponding to collagen biopolymer and HA, respectively. ¹⁵ Figure 3b illustrates the FTIR spectra of CFSP in the range of 4000–600 cm⁻¹. The characteristic peak at 1639 was attributed to C=O stretching vibrations due to the presence of collagen in the fish scale. ¹⁶

Furthermore, the various absorption peaks around 1018, 1024, and 1030 cm $^{-1}$ reveal the presence of HA and are attributed to $PO_4^{\ 3-}$ groups of HA. 17,18 The peaks observed at 1242 were attributed to amide III N—H bending. 19 The peaks at 1445 and 1389 cm $^{-1}$ were also attributed to the amide III C—N stretching vibrations, and the



characterizations of the carp fish scale powder: (a) x-ray diffraction, (b) Fourier transform infrared, and (c) thermogravimetric analysis. [Color figure can be viewed at wileyonlinelibrary.com]

FIGURE 4 (a, b) Morphology analysis of the carp fish scale powder using scanning electron microscopy.

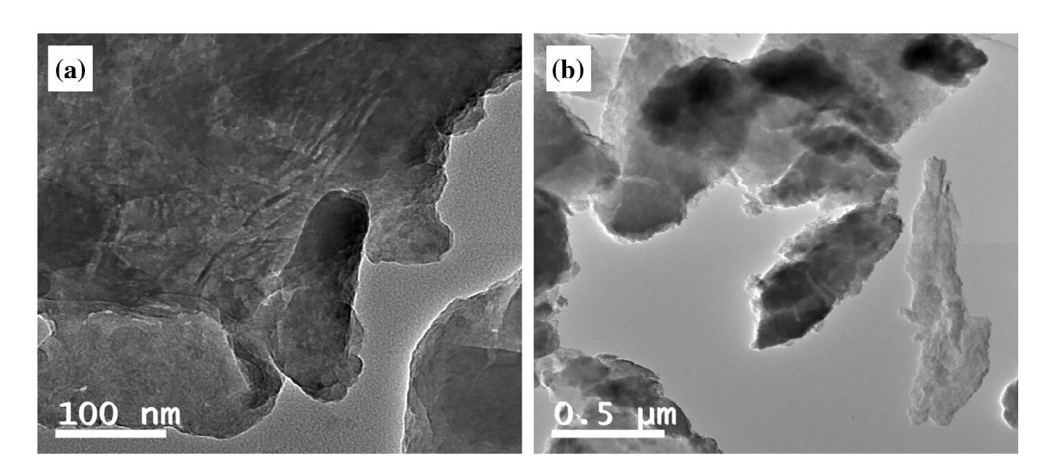


FIGURE 5 (a, b)
Transmission electron
microscopy image of carp fish
scale powder at different
magnifications.

peaks at 1532 cm⁻¹ are attributed to carbonate ions.²⁰ Figure 3c shows the TGA of the CFSP carried out at 800°C. The initial loss of 10% from the sample might be the presence of moisture, and from 290°C, considerable mass loss (~65%) was observed in the sample up to 800°C.

The SEM images of CFSP, obtained after cryo-milling, are shown in Figure 4a,b. The powder consists of irregular shapes and sizes of particles and includes elongated fibrous fragments inheriting the collagen fiber structure. The powders appear agglomerated and have fibrillary and granular structures on the surface. The collagen presence was confirmed by fibrils on the surface.

The morphological appearance and size were also examined by TEM, shown in Figure 5a,b. TEM image also showed agglomerated and irregularly shaped rod-like flake structures in micrometer size. These results match very well with TGA percentage of organic mass decomposition. The inorganic particle of HA was not clearly visible because of the large amount of organic content in the CFSP.

3.2 | Characterization of LLDPE/ CFSP films

3.2.1 | FTIR spectroscopy of biocomposite films

The FTIR spectrum of neat LLPDE, CFSP, 1 wt.% LLDPE/CFSP biocomposite films, as well as the SF₆ and O_2 plasma-treated fiber polymer biocomposite films in the range of 500–4000 cm⁻¹, are depicted in Figure 6. The characteristics of the absorbance band at 2914, 2848, 1462, and 715 cm⁻¹ were used to identify polyethylene's presence in all the films.^{23,24}

The peaks at 2916, 2848, and 1463 cm⁻¹ were attributed to C—H stretching, and the peak at 715 cm⁻¹ was attributed to the benzene derivative compound class. The characteristic peaks found in the CFSP at 1639 and 1242 cm⁻¹ were observed in biocomposite films, which shifted slightly to 1644 and 1237 cm⁻¹, respectively in

1 wt.% CFSPO $_2$ and 1 wt.% CFSPSF $_6$. It was observed that the plasma-treated films with O $_2$ and SF $_6$ were almost similar to the untreated films but the differences in the increasing intensities of the functional groups O—H, N—H, C=C, C—H, and C—O. It has been reported that the plasma treatment can increase the intensity of the carboxylic groups, amides, aromatic, and methyl groups resulting in the property enhancement in the plasma treated films. 17,25

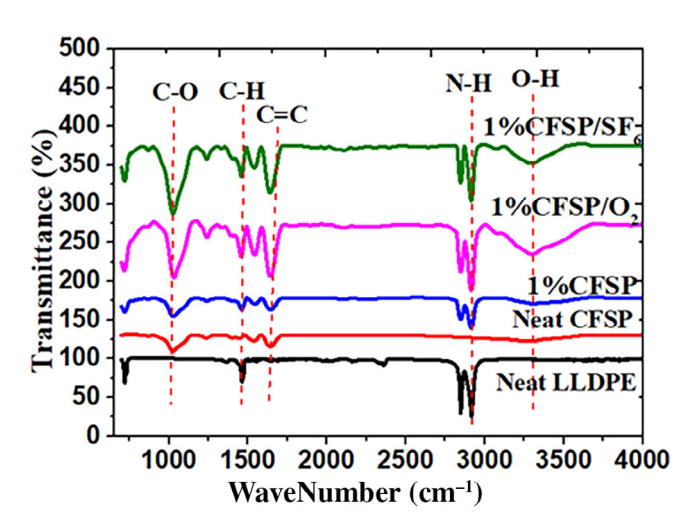


FIGURE 6 Fourier transform infrared spectrum obtained for the neat linear low-density polyethylene (LLDPE) films, neat carp fish scale powder (CFSP), and CFSP biocomposite films. [Color figure can be viewed at wileyonlinelibrary.com]

3.2.2 | Thermal analysis of LLDPE/CFSP biocomposite films

Figure 7a,b shows the TGA and the first derivative curve (DTG) curves obtained for the neat LLDPE, 1, 2, and 3 wt.% LLDPE/CFSP biocomposite films, and the SF₆ and O_2 plasma-treated 1% LLDPE/CFSP films.

The thermal properties of these biocomposite films analyzed using TGA are summarized in Table 2.

TABLE 2 Summary of different parameters obtained from the TGA curve of samples.

Samples	Initial decomposition temperature (°C)	Max. rate of decomposition temperature (°C)
Neat LLDPE	444.81	472.23
1% CFSP	467.55	490.75
2% CFSP	457.94	484.58
3% CFSP	459.90	485.20
1% CFSP/O ₂	475.78	498.16
1% CFSP/ SF ₆	476.89	500.02

Abbreviations: CFSP, carp fish scale powder; LLDPE, linear low-density polyethylene; TGA, thermogravimetric analysis.

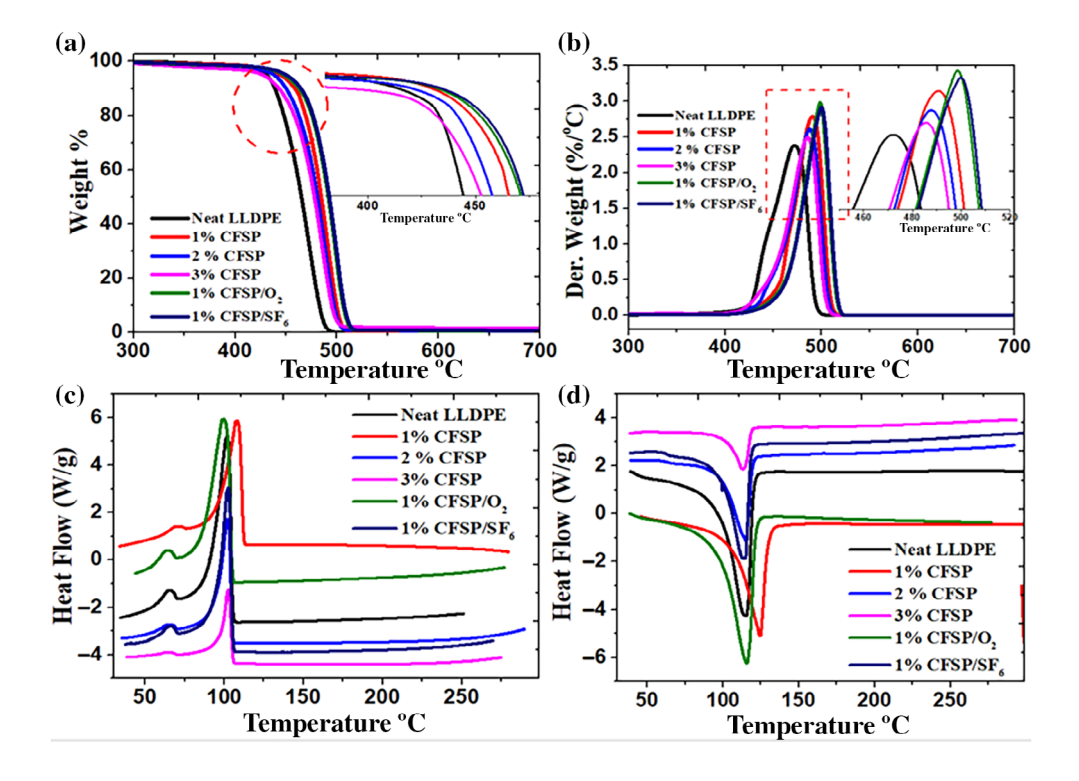


FIGURE 7 Thermograms obtained for LLDPE/CFSP films (a) thermogravimetric analysis (TGA) weight loss curves, (b) TGA derivative weight change, (c) differential scanning calorimetry (DSC) first heating cycle, and (d) DSC cooling cycle. [Color figure can be viewed at wileyonlinelibrary.com]

TABLE 3 Summary of different parameters obtained from DSC curves of samples.

Samples	Glass transition temperature (°C)	Melting temperature (°C)	Recrystallization temperature (°C)	Crystallinity %
Neat LLDPE	65.4	115.57	106.34	17.85
1% CFSP	69.6	124.38	107.96	29.75
2% CFSP	65.7	115.06	106.21	28.94
3% CFSP	64.9	113.32	102.41	23.83
1% CFSP/ O ₂	64.09	115.62	99.37	33.55
1% CFSP/ SF ₆	65.8	114.95	102.20	35.79

Abbreviations: CFSP, carp fish scale powder; DSC, differential scanning calorimetry; LLDPE, linear low-density polyethylene.

The initial decomposition temperature of the LLDPE/ CFSP biocomposite films was high compared with pure LLDPE polymer films. The maximum decomposition rate decreased with the increasing weight of FSP. 1 wt.% CFSP/LLDPE plasma-treated biocomposite films had a maximum initial decomposition temperature than those without plasma treatment. The increase in the thermal stability of the LLDPE/CFSP biocomposite films is attributed to the better reinforcement of the filler material in the polymer matrix. It was observed that 2 and 3 wt.% of CFSP in LLDPE films showed a reduction in the thermal stability compared to 1% CFSP biocomposite film probably because of aggregation of CFSP in polymer matrix at higher concentrations. The thermal stability of 1% CFSP/ LLDPE biocomposite with O2 and SF6 plasma treated showed significant improvement in thermal stability of 475.7 and 476.8°C, respectively. The maximum rate of thermal degradation was also significantly improved in O2 and SF6 plasma-treated 1% CFSP/LLDP with 498.16 and 500.02°C, respectively. The significant enhancement in the thermal properties of the plasma-treated biocomposite films with 1% CFSP is attributed to the surface modification of the polymer with functional groups in agreement with the FTIR spectrum of the biocomposite films shown in Figure 6

DSC thermograms are analyzed to study the polymer crystallinity properties of the blown films extruded. Figure 7c,d gives the thermograms obtained from DSC for the heating and cooling cycles at a heating rate of 10°C/min. The crystallinity of the films analyzed using the DSC curves showed the same trend as the maximum decomposition rate. The improved thermal stability of the films observed from TGA analysis can contribute to the improved crystallinity. Table 3 summarizes the data obtained for the biocomposite blown films using DSC analysis. The addition of the CFSP increased the

crystallinity % from 17.85 in the neat film to 29.75 in the 1 wt.% biocomposite films. The increase in crystallinity was attributed to the nucleation effect. The CFSP acts as a nucleating agent that provides sites for initiating crystallization, thereby enhancing the crystalline region's nucleation process and formation. The nucleation effect facilitates crystalline structure growth and improves the biocomposite film's overall crystallinity. The crystallinity slightly decreased with increasing loading content of CFSP. However, the crystallinity % increased significantly with 1 wt.% SF₆ plasma-treated biocomposite film has the highest crystallinity % of 35.79. The plasma treatment initiated a crosslinking reaction, which increased the overall crystallinity of the films. The crystallinity was calculated from the following Equation (1)

$$\chi_{\rm c} = \frac{\Delta H_{\rm m} - \Delta H_{\rm c}}{\Delta H_{\rm f}},\tag{1}$$

where $X_{\rm c}$ is crystallinity, $\Delta H_{\rm m}$ and $\Delta H_{\rm c}$ are the enthalpy of melting and cold crystallization, respectively. $\Delta H_{\rm f}$ is the enthalpy of fusion of 100% crystalline sample (293 J/g for LLDPE). Table 2 summarizes the data obtained for the thermal properties of the biocomposite films using TGA and DSC analysis.

3.2.3 | Tensile test analysis

The tensile properties of the prepared films are shown in Figure 8 and results are summarized in Table 4. The addition of CFSP slightly decreased the tensile strength of the biocomposite films from 5.30 to 4.95 MPa for one wt.% loading content. The tensile strength decreased with increasing wt.% of CFSP, similar to the result Danjaji et al.²³ and Reesha et al.²⁶ obtained when they used

starch and chitosan as a bio filler in LLDPE. The decrease in the tensile strength is due to aggregation and organic content (collagen) uneven dispersion of CFSP in the LLDPE matrix. The hydrophilic nature of CFSP increases its tendency to agglomerate. The accumulation causes uneven dispersion and acts as stress concentration sites. Cracks initiate and propagate from the stress-concentrated site, reducing the tensile strength.

However, the modulus of the biocomposite films increased with the increasing loading content of CFSP and showed good agreement with literature on LLDPE using biomaterial as filler contents. The increase in modulus is due to the stiffness of CFSP being higher than the LLDPE polymer matrix. Aradhyula et al. used a twin-screw extrusion technique to fabricate a biocomposite of catla fish scale as a reinforcing agent in polypropylene. They reported that the tensile strength and elongation-at-break decreased with increasing catla fish scale content. However, Young's modulus improved significantly. CFSP has a fibril nature with high stiffness.

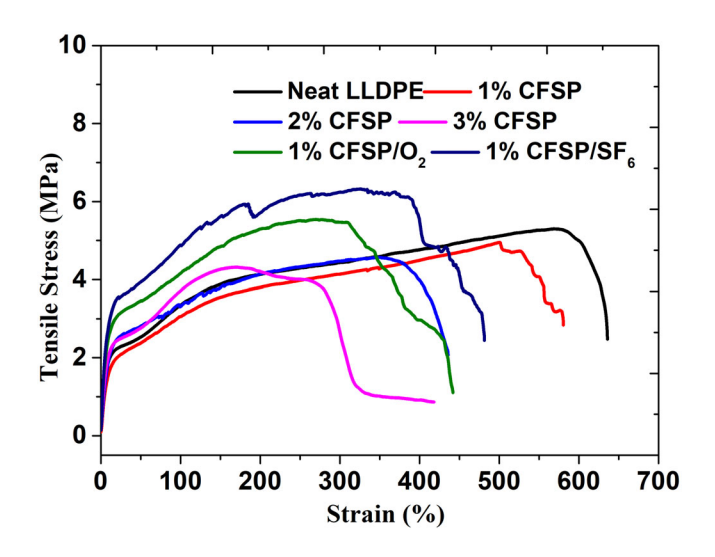


FIGURE 8 Showing the stress-strain graph of CFSP/LLDPE films. CFSP, carp fish scale powder; LLDPE, linear low-density polyethylene. [Color figure can be viewed at wileyonlinelibrary.com]

TABLE 4 Tensile test results of various biocomposite films prepared.

Samples	F _{max} (MPa)	E _{mod} (GPa)	Elongation at break (%)
Neat LLDPE	5.30	0.012	635
1% CFSP	4.95	0.014	580
2% CFSP	4.56	0.017	433
3% CFSP	4.31	0.019	418
1% CFSP/O ₂	5.54	0.020	441
1% CFSP/SF ₆	6.32	0.023	481

Abbreviations: CFSP, carp fish scale powder; LLDPE, linear low-density polyethylene.

Rigid fillers are generally known to increase the modulus of the matrix in which they are dispersed. 30 Furthermore, the strength and modulus of the plasma-modified fiber polymer biocomposite films showed an increment. Table 4 summarizes the tensile properties of the blown film samples prepared for this study. SF_6 plasma-treated biocomposite had the highest tensile strength and modulus of 6.32 MPa and 0.23 GPa. The increase in the tensile strength and modulus is attributed to the plasma treatment inducing crosslinking reaction, creating a molecular network structure that strengthens the biocomposite films and further improves its strength and modulus. 31,32 Table 4 lists the tensile properties of the blown film samples prepared for this study.

3.2.4 | SEM fracture of surfaces

SEM micrographs of the fracture surfaces of the films are shown in Figure 9. Figure 9a shows the fracture surface of the neat LLDPE films with a smooth surface due to the rapid propagation of cracks. The SEM micrographs in Figure 9b revealed agglomerated CFSP creating voids at the surface fracture of the 1 wt.% LLDPE/CFSP biocomposite films because of slow crack propagation. The drop in the tensile strength of the biocomposite films results from the aggregation that has created voids at the surface of the fractured films, as revealed by the SEM. Figure 9c,d shows that the voids were not observed in SF₆ and O₂ plasma-treated fiber polymer biocomposite films. The plasma treatment increased the crystallinity by causing a crosslinking reaction, improving the adhesion between CFSP and LLDPE and ultimately improving the tensile strength of the plasma-modified fiber polymer biocomposite films.

3.2.5 | Biodegradability test

XRF analysis showed increased phosphorus and calcium mass percent in the soil after the natural soil

FIGURE 9 Showing scanning electron microscope surface fracture of (a) neat LLDPE, (b) 1% CFSP, (c) 1% CFSP/O₂, and (d) 1% CFSP/ SF₆. CFSP, carp fish scale powder; LLDPE, linear low-density polyethylene.

TABLE 5 Showing elemental mass percentages of the samples used for the biodegradability test.

Sample	Phosphorus (mass%)	Calcium (mass%)
Soil before burial	0.166	0.112
Soil after burial of 1% CFSP	0.182	0.233
Soil after the burial of 1% CFSP/O ₂ film	0.180	0.243
Soil after the burial of 1% CFSP/SF ₆ film	0.179	0.233

biodegradability test, indicating that the biocomposite disintegrates into the soil. The film collected after the 90-day burial test is given in Figure 2b. It was observed that no visible changes were observed on the films after 90 days. However, the XRF analysis showed an increase in phosphorous and calcium mass percentage in the soil.

Table 5 shows the mass percentage of phosphorous and calcium analyzed in the soil before and after the biocomposite film burial test. Before the burial test, the mass percentages of phosphorus and calcium were 0.166 and 0.112, respectively. The change in elemental mass percent in the soil after the burial test is attributed to the disintegration of calcium and phosphate ions in HA $(Ca_{10}(PO_4)_6(OH)_2)$.

4 | CONCLUSIONS

The successful preparation of CFSP from raw CFS yielded irregularly shaped particles with an average size of $0.5~\mu m$, as confirmed by TEM and SEM analysis. Characterization via FTIR identified the presence of collagen and HA within the powder. The incorporation of CFSP into biocomposite thin films notably enhanced their thermal properties by acting as a nucleating agent, facilitating

the initiation of crystallization and augmenting the formation of crystalline regions. However, an increase in CFSP loading led to reduced tensile strength due to particle agglomeration, resulting in stress concentration sites that initiated cracks, impacting the overall strength. Notably, SF₆ plasma-treated biocomposite-fabricated thin films exhibited superior characteristics, boasting a maximum decomposition rate of 500.02°C, a crystallinity index of 35.79, and tensile strength and modulus of 6.32 MPa and 0.023 GPa, respectively. These enhancements stemmed from the crosslinking reactions induced by plasma treatment, improving the mechanical properties. Moreover, soil analysis via XRF before and after exposure to biocomposite films revealed an increase in phosphorus and calcium mass percent, indicative of the biocomposite's degradation within the soil. The HA(-Ca₁₀(PO₄)₆(OH)₂) present in the CFSP that is used for the fabrication of the biocomposite influenced the disintegration of phosphorus and calcium into the soil. This finding suggests degradation of the biocomposite compared with neat LLDPE film, which does not degrade. In summation, the utilization of CFSP as a sustainable natural bio filler in the production of green materials, when integrated into LLDPE matrices offers promising potential for developing environmentally friendly materials with improved structural integrity.

AUTHOR CONTRIBUTIONS

Vijaya K. Rangari: Conceptualization (equal); data curation (equal); resources (lead); writing – original draft (equal); writing – review and editing (equal). Matthew Bonzu Ackah: Data curation (lead); formal analysis (lead); investigation (lead); methodology (equal); writing – original draft (equal). Radhika Panickar: Formal analysis (equal); writing – original draft (equal); writing – review and editing (equal).

ACKNOWLEDGMENTS

The authors would like to acknowledge the financial support from AL-EPSCoR #1655280, NSF CREST #1735971, and MRI# 2117242.

DATA AVAILABILITY STATEMENT

The data that support the findings of this study are available from the corresponding author upon reasonable request.

ORCID

Vijaya K. Rangari https://orcid.org/0000-0002-3962-1686

REFERENCES

- S. Kannan, Y. Gariepy, G. S. V. Raghavan, Waste Manage. 2017, 65, 159.
- [2] A. Santana, C. Piccirillo, S. I. A. Pereira, R. C. Pullar, S. M. Lima, P. M. L. Castro, J. Environ. Chem. Eng. 2019, 7, 103403.
- [3] S. Lv, L. Hu, C. Xia, M. B. Cabrera, Y. Guo, C. Liu, L. You, J. Cleaner Prod. 2021, 288, 125682.
- [4] E. Alabaraoye, M. Achilonu, H. Robert, J. Polym. Environ. 2018, 26, 2207.
- [5] M. Gharehbaghi, M. Dehghani-Firouzabadi, Azadfallah, J. Polym. Environ. 2020, 12, 3273.
- [6] M. Jawaid, H. P. S. Abdul Khalil, A. Hassan, R. Dungani, *Polymers* 2019, 11, 1834.
- [7] M. A. Khan, S. M. J. Zaidi, M. A. Khan, R. A. Khan, J. Cleaner Prod. 2019, 230, 1289.
- [8] K. Ramesh Babu, V. Jayakumar, G. Bharathiraja, S. Madhu, Mater. Todav: Proc. 2020, 22, 416.
- [9] M. Wang, R. Joseph, W. Bonfield, Biomaterials 1998, 19, 2357.
- [10] A. A. Majhooll, I. Zainol, C. N. A. Jaafar, H. A. Alsailawi, M. Z. Hassan, M. Mudhafar, A. A. Majhool, A. Asaad, J. Chem. Eng. 2019, 13, 112.
- [11] A. Ogino, S. Noguchi, N. Masaaki, Adv. Mater. Res 2011, 22, 896.
- [12] S. Yoshida, K. Hagiwara, T. Hasebe, A. Hotta, Surf. Coat. Technol. 2013, 233, 99.
- [13] H.-S. Choi, Y.-S. Kim, Y. Zhang, S. Tang, S.-W. Myung, B.-C. Shin, Surf. Coat. Technol. 2004, 182, 55.
- [14] S.-D. Lee, G.-H. Hsiue, P. C.-T. Chang, C.-Y. Kao, *Biomaterials* 1996, 17, 1599.
- [15] S. Sartori, A. Rechichi, G. Vozzi, M. D'Acunto, E. Heine, P. Giusti, G. Ciardelli, React. Funct. Polym. 2008, 68, 809.
- [16] P. G. Allison, R. I. Rodriguez, R. D. Moser, B. A. Williams, A. R. Poda, J. M. Seiter, B. J. Lafferty, A. J. Kennedy, M. Q. Chandler, J. Visualized Exp. 2014, 89, 51535.
- [17] S. Kongsri, K. Janpradit, K. Buapa, S. Techawongstien, S. Chanthai, Chem. Eng. J. 2013, 215, 522.
- [18] S. Paul, A. Pal, A. R. Choudhury, S. Bodhak, V. K. Balla, A. Sinha, M. Das, Ceram. Int. 2017, 43, 15678.
- [19] C.-S. Wu, W. Dung-Yi, S.-S. Wang, ACS Appl. Bio Mater. 2020, 4, 462.
- [20] J. Athinarayanan, V. S. Periasamy, A. A. Alsha, *Mater. Sci. Eng. C* 2020, 117, 111313.
- [21] T. Safronova, V. Vorobyov, N. Kildeeva, T. Shatalova, O. Toshev, Y. Filippov, A. Dmitrienko, O. Gavlina, O. Chernega, E. Nizhnikova, M. Akhmedov, E. Kukueva, K. Lyssenko, *Ceramics* 2022, 5, 484.
- [22] J. Praveenkumara, P. Madhu, T. Girijappa, Y. Gowda, R. S. Mavinkere, S. Suchart, *J. Nat. Fibers* **2022**, *19*, 4132.
- [23] I. D. Danjaji, R. Nawang, U. S. Ishiaku, H. Ismail, Z. A. Mohd. Ishak, J. Appl. Polym. Sci. 2001, 79, 29.
- [24] M. C. Silva, G. Petraconi, R. R. R. Cecci, A. A. Passos, W. F. do Valle, B. Braite, S. R. Lourenço, F. Gasi, *Polymers* 2021, 13, 1969.
- [25] G. Wu, M. Feng, H. Zan, RSC Adv. 2015, 5, 44636.
- [26] K. V. Reesha, S. K. Panda, J. Bindu, T. O. Varghese, Int. J. Biol. Macromol. 2015, 79, 934.

- [27] Z. M. Razi, M. R. Islam, M. Parimalam, Polym. Test. 2019, 74, 7.
- [28] P. Raja Sekaran, S. Ganesh Kumar, A. J. Singh J, J. Vairamuthu, *Mater. Today: Proc.* **2020**, *33*, 2214.
- [29] A. T. Vasu, B. Da, R. A. Babul, J. Yeau-Ren, C. Murthy, E. R. Sadiku, M. Ramakrishna, Adv. Compos. Mater 2020, 29, 115.
- [30] A. Chapiro, Nuclear Instruments and Methods in Physics Research Section B: Beam Interactions with Materials and Atoms, Vol. 105 **1995**, p. 5.
- [31] H. Dong, L. Bogg, C. Rehnberg, V. Diwan, Health Policy 1999, 48, 29

[32] B. Tissington, G. Pollard, I. M. Ward, Compos. Sci. Technol. 1992, 44, 185.

How to cite this article: M. B. Ackah, R. Panickar, V. K. Rangari, *J. Appl. Polym. Sci.* **2024**, *141*(19), e55352. https://doi.org/10.1002/app.55352